

More about Q-ball with elliptical orbit

Fuminori Hasegawa,^{1,2,*} Jeong-Pyong Hong,^{3,†} and Motoo Suzuki^{1,2,‡}

¹*ICRR, University of Tokyo, Kashiwa, Chiba 277-8582, Japan*

²*Kavli IPMU (WPI), UTIAS, University of Tokyo, Kashiwa, Chiba 277-8583, Japan*

³*Center for Theoretical Physics, Department of Physics and Astronomy, Seoul National University, Seoul 08826, Korea*

(Dated: May 17, 2022)

Q-balls formed from the Affleck-Dine field have rich cosmological implications and have been extensively studied from both theoretical and simulational approaches. From the theoretical point of view, the exact solution of the Q-ball was obtained and it shows a circular orbit in the complex plane of the field value. In practice, however, it is reported that the Q-ball that actually appears after the Affleck-Dine mechanism has an *elliptical* orbit and carries larger energy per unit $U(1)$ charge than the well-known solution with a circular orbit, which is expected to relax into the Q-balls with circular orbits. We call them “elliptical” Q-balls. In this paper, we investigate properties of the elliptical Q-ball by 3D lattice simulation and derive the solution for the elliptical Q-ball by the semi-analytical way. These analyses, for example, enable us to discuss how energy excitation depends on the ellipticity of the Q-ball.

I. INTRODUCTION

Q-ball is a non-topological soliton in a complex scalar field theory with a global $U(1)$ symmetry [1]. The solution corresponds to the spherically symmetric field configuration minimizing the energy of the system with the fixed $U(1)$ charge. Such a solution exists for the potential $V(\phi)$ of the complex scalar field ϕ if $V(\phi)/|\phi|^2$ has the minimum at $\phi \neq 0$. One of the characteristics of the solution is that the configuration of ϕ has time dependence and the orbit of ϕ in the complex plane is a true circle.

The formation of the Q-ball has been studied analytically and numerically in some extensions of the standard model. For example, in the supersymmetric extension of the standard model, some scalar condensates with the baryon number form Q-balls after Affleck-Dine baryogenesis [2–14]. There, the initial configuration of the complex scalar field is set to be the coherently oscillating state in the complex plane. Due to the instability of such a state, the initial fluctuation of the scalar field grows and eventually develops into the Q-balls.

One non-trivial result from the numerical analysis is the discovery of excited states of Q-balls [14, 15].¹ The excited state has larger energy compared to the energy minimum solution with the same charge. The configuration of the complex scalar in the excited state draws an elliptical orbit, while the orbit of a genuine Q-balls is a true circle. We call excited Q-balls as the “elliptical” Q-balls and genuine ones as the ground state Q-balls. It is numerically shown that the elliptical Q-balls are semi-stable at least [14] and they are considered as the “transients”, which appear during the formation of the circular Q-balls.

Even though the formation of the elliptical Q-balls was pointed out, their properties were not pursued sufficiently. For instance, in the numerical simulation, there is no detailed investigation for how the energy excitation depends on the ellipticity. The theoretical explanation on the elliptical Q-ball solution is also not present.²

In this paper, we investigate the properties of the elliptical Q-ball in numerical and analytical ways. We first perform 3D lattice simulations, and present the spatial profiles and field orbits of the elliptical Q-balls and so on. Next, we derive the elliptical Q-ball solution and discuss its properties in a semi-analytical way. In particular, we obtain the relation among the energy, charge, radius, and ellipticity of the Q-ball, which will be shown to be in agreement with the lattice simulation in good precision. We also point out that the elliptical Q-ball is an unstable solution and will decay into more stable, that is, mildly elliptical Q-balls in a finite time scale. While our study on the elliptical Q-balls is from theoretical curiosity, the theory can be used for the extension of the other non-topological solitons, *e.g.* oscillon/I-ball [18–26] and boson star [27, 28]. For instance, Refs. [29, 30], suggest that oscillon/I-ball and boson star can be understood as Q-ball solutions associated with the particle number $U(1)$ charge, which will make it possible to derive some extended solutions of such non-topological solitons, using our extended theory of the Q-balls.

* e-mail: fuminori@icrr.u-tokyo.ac.jp

† e-mail: hjp0731@snu.ac.kr

‡ e-mail: m0t@icrr.u-tokyo.ac.jp

¹ In Ref. [15], the excited state is named “Q-axitons”.

² It should be noted that the “elliptical” Q-ball is different from the excited state solution that is discussed in *e.g.* Refs. [16, 17]. The radial excitation with nodes [16, 17] and the (non-spherical symmetric) angular excitation [16] of the Q-ball solution are studied as possible forms of the excitation. However, the Q-balls produced in the lattice simulation seem to have no nodes and almost spherical symmetric (See Sec. III for more details.).

The paper is organized as follows. In Sec. II, we review the ground state Q-ball solution and its properties. In Sec. III, we show the formation of the elliptical Q-balls through the classical lattice simulation and discuss their properties. In Sec. IV, we derive the elliptical Q-ball solution by semi-analytical approaches and compare the solution with the results from the simulation. The final section is devoted to our conclusion.

II. REVIEW: GROUND STATE Q-BALL SOLUTION

In this section, we review the ground state Q-ball.³

Let us consider the theory of a complex scalar field ϕ . The Lagrangian density is given by

$$\mathcal{L} = \partial_\mu \phi \partial^\mu \phi^* - V(\phi). \quad (1)$$

Here, $V(\phi)$ is a potential with the $U(1)$ symmetry, which is invariant under the phase rotation of ϕ . The Noether charge of this $U(1)$ symmetry is given by

$$Q = \frac{1}{i} \int d^3x (\phi^* \dot{\phi} - \dot{\phi}^* \phi). \quad (2)$$

The energy is represented as

$$E = \int d^3x \left[\dot{\phi} \dot{\phi}^* + \nabla \phi \nabla \phi^* + V(\phi) \right]. \quad (3)$$

To figure out the ground state Q-ball solution, let us consider the energy minimum condition for a fixed charge. Using the method of Lagrange multipliers, one must find an extremum of

$$E_\omega = \int d^3x \left[\dot{\phi} \dot{\phi}^* + \nabla \phi \nabla \phi^* + V(\phi) \right] + \omega \left(Q - \int d^3x i(\dot{\phi}^* \phi - \phi^* \dot{\phi}) \right). \quad (4)$$

$$= \int d^3x \left[|\dot{\phi} - i\omega \phi|^2 + |\nabla \phi|^2 - \omega^2 |\phi|^2 + V(\phi) \right] + \omega Q, \quad (5)$$

where ω is a Lagrange multiplier. From the first term of the integrand in the second line, the time-dependent part of ϕ is minimized for the choice

$$\phi(\mathbf{x}, t) = \frac{1}{\sqrt{2}} \Phi(\mathbf{x}) e^{i\omega t}. \quad (6)$$

Note that this formula indicates that the orbit in the complex plane is a true circle. Then, the Eq. (4) is reduced to

$$E_\omega = \int d^3x \left[\frac{1}{2} (\nabla \Phi)^2 - \frac{1}{2} \omega^2 \Phi^2 + V(\Phi) \right] + \omega Q. \quad (7)$$

As the extremum condition, we then obtain the equation of motion for $\Phi(\mathbf{x})$

$$\frac{d^2 \Phi}{dr^2} + \frac{2}{r} \frac{d\Phi}{dr} + \omega^2 \Phi - \frac{\partial V(\Phi)}{\partial \Phi} = 0, \quad (8)$$

where we assume that Φ is spherically symmetric in the position space and r is the radial coordinate. This equation of motion is the same as the one from the Lagrangian density in Eq. (1) by using the ansatz in Eq. (6). From the finiteness of the energy and the continuity of the solution, one imposes the boundary condition,

$$\Phi'(0) = 0, \quad \Phi(\infty) = 0. \quad (9)$$

One can find the solution of this equation by the analogy with the system where the scalar field rolls down with the potential $\omega^2 \Phi - \partial V(\Phi)/\partial \Phi$ under the expansion of the universe. It must be noted that the existence of the solution highly depends on the form of the scalar potential $V(\Phi)$. The condition for the existence of the solution is given by

$$\exists \omega \text{ which satisfies } \text{Min} \left[\frac{2V(\Phi)}{\Phi^2} \right] < \omega^2 < \left. \frac{2V(\Phi)}{\Phi^2} \right|_{\Phi=0} \quad (\equiv m_\Phi^2). \quad (10)$$

This condition claims that $V(\Phi)$ must be ‘‘shallower’’ than the quadratic. For example, $V(\Phi) \propto \Phi^{1.9}$ satisfies this condition and hence the solution exists. Since the existence of this lump solution is ensured by the conservation of the total charge Q , it is called ‘‘Q-ball’’.

³ See *e.g.* Ref. [31] and references therein for review.

Q-ball solution in gravity-mediation potential

For the later purpose, let us discuss the Q-ball solution for a specific potential. It is known as the “gravity-mediation potential”,

$$V(\phi) = m^2 |\phi|^2 \left[1 + K \ln \left(\frac{|\phi|^2}{M_*^2} \right) \right], \quad (11)$$

where M_* is the renormalization scale defining the mass parameter, m , of the complex scalar field. The constant K is for example determined as $K = -0.01 \sim -0.1$ by the spectrum of the minimal supersymmetric standard model. Throughout this paper, we take,

$$K = -0.1. \quad (12)$$

The equation of motion under the gravity-mediation potential is numerically solved and it is shown that the solution is well approximated by the Gaussian spatial profile [9],

$$\Phi(r) = \Phi(0) e^{-r^2/R^2}. \quad (13)$$

By substituting this into the Eq. (8), one obtains the following relation,

$$\omega \simeq m \left[1 + 2|K| - |K| \ln \left(\frac{\Phi(0)^2}{2M_*^2} \right) \right]^{1/2} \sim m, \quad (14)$$

$$R \simeq \left(\frac{2}{|K|} \right)^{1/2} m^{-1}. \quad (15)$$

Then, the charge and the energy is obtained as

$$Q \simeq \left(\frac{\pi}{2} \right)^{3/2} m \Phi(0)^2 R^3, \quad (16)$$

$$E \simeq mQ. \quad (17)$$

It is confirmed that these properties agree with the full numerical and allow us qualitative discussion. We stress that the most important feature of the ground state Q-ball is the “dispersion relation”

$$E/Q \simeq m. \quad (18)$$

As we will see later, the Q-balls formed in the realistic situation has elliptical orbits and no longer follow this relation. In the following, we redefine the parameters as

$$\begin{aligned} mt &\rightarrow t \\ mr &\rightarrow r \\ mR &\rightarrow R \\ \phi/M_* &\rightarrow \phi \\ \omega/m &\rightarrow \omega \\ Em/M_*^2 &\rightarrow E \\ Qm^2/M_*^2 &\rightarrow Q. \end{aligned} \quad (19)$$

Then, the charge is the same as the formula in Eq. (2) and the energy of the system is rewritten simply as

$$E = \int dx^3 \left[\dot{\phi} \dot{\phi}^* + \nabla \phi \nabla \phi^* + |\phi|^2 (1 + K \ln |\phi|^2) \right]. \quad (20)$$

The dispersion relation is

$$E/Q \simeq 1. \quad (21)$$

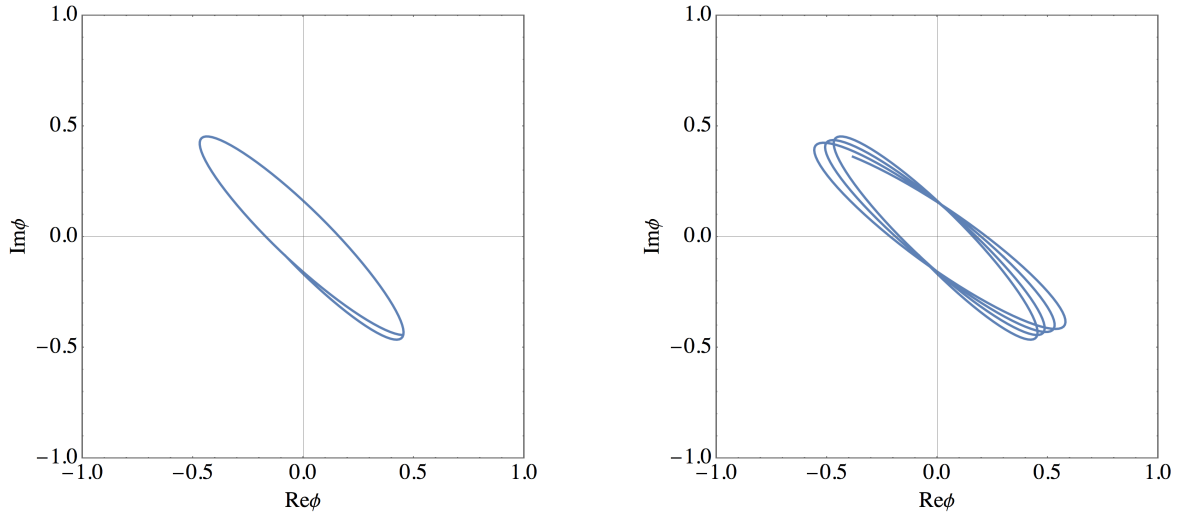


FIG. 1. The orbit of the elliptical Q-ball produced in the lattice simulation for about one oscillation time (left) and about three oscillation times (right).

III. NUMERICAL SIMULATION

In this section, we perform a simulation in the gravity-mediation potential and show the formation and properties of the elliptical Q-balls.

In our analysis, we use the package PyCOOL [32], which we modified for our analysis. The PyCOOL is an object-oriented Python program that uses GPU(s) for simulating the scalar field dynamics in the early universe and performs the 3D simulations.

Following Ref. [32], we use $N_{\text{grid}} = 128^3$, $L = 8$, $t_i = 100$, $t_f = 5000$, and $\Delta\tau = 0.005$.⁴ There, t_i , t_f are initial and final time, and τ is the conformal time, respectively.

We assumed the matter-domination after the inflation⁵ and set the initial scale factor unity: $a(t = t_i) = 1$. As the initial condition for the homogeneous AD field, we take

$$\phi(t = t_i) = 1, \quad (22)$$

$$\frac{d\phi}{dt}(t = t_i) = i\epsilon_{\text{ini}}, \quad (23)$$

where ϵ_{ini} represents the initial ellipticity of the orbit in the complex plane. We also give the initial Gaussian fluctuation, though the eventual phenomena are known to be irrelevant to this initial condition on the fluctuation, except for the formation time of the objects.

As the result of our simulation, we confirmed that the non-linear lumps are formed at $t_{\text{form}} \sim 8 \times 10^2$, which are stable, that is, do not decay into the scalar waves, until the final time. We identified the localized objects as the excited Q-balls by fitting the semi-analytical profiles as we will discuss later.

First of all, let us confirm that the produced Q-ball has an elliptical orbit. In Fig. 1, we present the orbit at the center of the lump, which is plotted around the final time $t_f = 5000$. We can see that it is indeed an ellipse that has a rotating axis (left figure). We also find that the orbit itself slightly rotates around the origin when we observe the orbit for a longer time (right figure), whose behavior will be explained in the next section. The normalization of figures in the following section is the one in Eq. (19).

In Fig. 2, we also present the charge density profile of the lump with the maximal charge. The horizontal axes for the three figures denote the three space coordinates. The vertical axis is the charge density. The profile fits well to the gaussian profile. It should be noted that the charge density profile of the elliptical Q-ball is almost spherically symmetric. We also note that there are no nodes for the profile. Those properties suggest that the elliptical Q-ball is different from the excited states discussed in Refs. [16, 17].

⁴ For the parameters before the redefinition in Eq. (19), $N_{\text{grid}} = 128^3$, $Lm = 8$, $t_i = 100m^{-1}$, $t_f = 5000m^{-1}$, and $m\Delta\tau = 0.005$.

⁵ We also performed the simulation in the Minkowski case, but identifying the profile and the elliptical behavior was difficult due to the contamination by undamping higher modes.

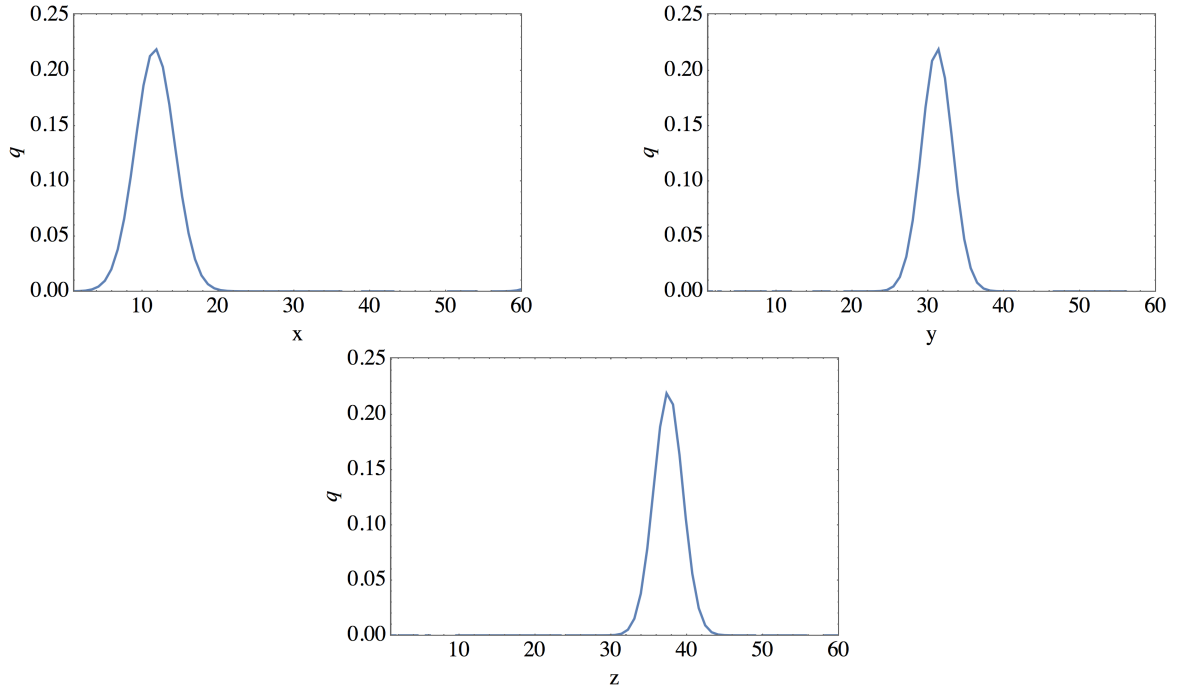


FIG. 2. The charge density profile for the Q-ball in Fig. 1. The labels (x, y, z) denote the three-dimensional space coordinates. Notice that we focus on the location of a Q-ball, and thus the horizontal axes only vary from 0 to 60.

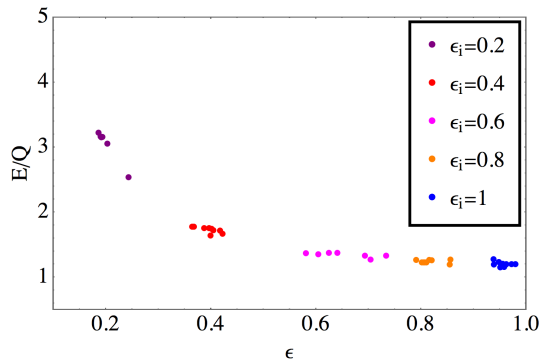


FIG. 3. The dispersion relation E/Q obtained from the Q-ball obtained in the lattice simulation. The difference in color denotes the difference of the initial parameter ϵ_i .

Next, let us see the dispersion relation of the elliptical Q-ball. In Fig. 3, we plot the relation between E/Q and ϵ of the Q-balls with the charge of $10 \lesssim Q \lesssim 100$, where ϵ is defined by the short axis of the ellipse divided by the long axis of the ellipse. The difference in color of the dots denotes the difference in the initial condition. We vary the initial ellipticity ϵ_{ini} from 0.2 to 1.

We confirm that E/Q of the elliptical Q-balls is larger than those of the ground state Q-balls. In other words, it is shown that the energy of the elliptical Q-balls is larger than that of the ground state Q-balls for a fixed charge. This time we have run the simulations with $N_{\text{grid}} = 64^3$ in order to save the time of computation. We confirmed for several samples that there is no essential difference from the case of $N_{\text{grid}} = 128^3$ in the plot.

IV. SEMI-ANALYTICAL DERIVATION OF ELLIPTICAL Q-BALL SOLUTION

As we discussed in the previous section, the properties of the elliptical Q-balls apparently deviate from those of the ground state Q-ball solution. The elliptical Q-balls have larger E/Q compared to the ground state Q-balls.

Furthermore, the elliptical Q-balls are (semi-)stable as shown in the previous section or the previous works.

In this section, we derive the solution for the elliptical Q-ball. Obtaining the exact solution is more subtle since the variables cannot be separated like Eq. (6). However, we figure out the elliptical Q-ball solution by using two types of approximation. As in the previous section, we focus on the gravity mediation potential,

$$V(\phi) = |\phi|^2 [1 + K \ln(|\phi|^2)]. \quad (24)$$

In the next section, we compare those solutions with the results from the simulations.

A. Method 1: complete ellipse approximation

As we have seen in Fig. 1, the orbit of the elliptical Q-ball is almost closed during an oscillation. Thus, in method 1, let us approximate that the orbit of ϕ is a complete ellipse, that is,

$$\phi = \frac{1}{\sqrt{2}} \Phi(\mathbf{x}) P(\omega t), \quad P(\omega t) = \sqrt{\frac{1}{\epsilon}} (\cos \omega t + i \epsilon \sin \omega t), \quad (25)$$

where ϵ is the ellipticity parameter. Here, we take $0 < \epsilon \leq 1$. For $\epsilon = 1$, the ansatz is nothing but the one for the ground state Q-ball in Eq. (6).

Under this ansatz, the total charge Q is given by

$$Q = \int d^3x \omega \Phi(\mathbf{x})^2. \quad (26)$$

Apparently, the charge is time-invariant under the above ansatz.

The equation of motion for ϕ is

$$-\ddot{\phi} + \frac{d^2 \phi}{dr^2} + \frac{2}{r} \frac{d\phi}{dr} - \frac{\partial V(\phi)}{\partial \phi^*} = 0. \quad (27)$$

By inserting the ansatz, multiply by $P(\omega, t)$, time average over the period $2\pi/\omega$, then we obtain

$$\frac{d^2 \Phi}{dr^2} + \frac{2}{r} \frac{d\Phi}{dr} + \omega^2 \Phi - \frac{\partial \bar{V}(\Phi)}{\partial \Phi} = 0. \quad (28)$$

Here, $\bar{V}(\Phi)$ is the time-averaged potential,

$$\bar{V}(\Phi) = \frac{1}{2} \Phi^2 (1 + c(\epsilon) + K \ln \Phi^2), \quad (29)$$

where

$$c(\epsilon) = \frac{2\epsilon}{1 + \epsilon^2} \frac{K}{2\pi/\omega} \int_0^{2\pi/\omega} |P(\omega t)|^2 \ln \left(\frac{1}{2} |P(\omega t)|^2 \right) \simeq K \ln \left(\frac{1 + \epsilon^2}{2\epsilon} \right). \quad (30)$$

The equation in Eq. (28) is identical to that of the ground state Q-ball in Eq. (7). Therefore, we can use the Gaussian approximation in Sec. II and obtain the following properties,

$$\omega \simeq \left[1 + 2|K| - |K| \ln \left(\frac{\Phi(0)^2}{2} \right) \right]^{1/2} \sim 1, \quad (31)$$

$$R \simeq \left(\frac{2}{|K|} \right)^{1/2}, \quad (32)$$

$$Q \simeq \left(\frac{\pi}{2} \right)^{3/2} \Phi(0)^2 R^3. \quad (33)$$

The dispersion relation is also given by

$$\bar{E}/Q \simeq \frac{1 + \epsilon^2}{2\epsilon}, \quad (34)$$

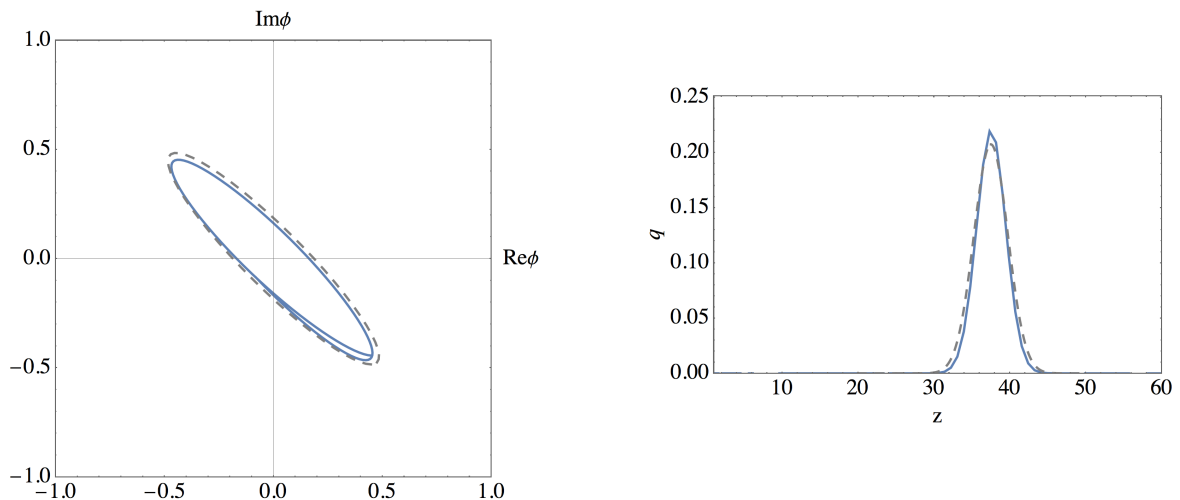


FIG. 4. Fitting in method 1. The gray dashed line is the orbit and the charge density profile from method 1 in the left and the right figures, respectively. The blue line is the same as the one in Fig. 1. Here, we take $\epsilon = 0.2$, $\omega = 1.149$.

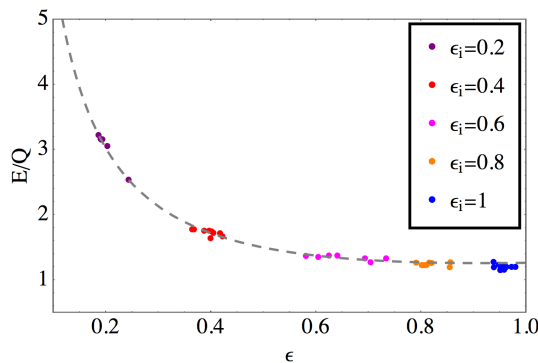


FIG. 5. The dispersion relations obtained from the lattice simulation and from method 1. The gray dotted line is E/Q for $Q = 50$. The data from the simulation is the same as the ones in Fig. 3.

for the time-averaged energy,

$$\bar{E} = \frac{1 + \epsilon^2}{2\epsilon} \int dx^3 \left[\frac{1}{2} \omega^2 \Phi^2 + \frac{1}{2} (\nabla \Phi)^2 + \frac{1}{2} \Phi^2 (1 + c(\epsilon) + K \ln \Phi^2) \right]. \quad (35)$$

The dispersion relation in Eq. (34) is different from that of circular Q-ball in Eq. (21). While elliptical Q-ball solution coincides with the circular Q-ball solution for $\epsilon = 1$, it carries larger energy per unit charge than the circular one for $\epsilon \neq 1$. Therefore, we can regard the elliptical Q-ball as a kind of “excited state” of the Q-ball.

Comparing with simulation result

Let us first determine the variables ω and ϵ from the orbit in Fig. 1. From the figure, the ellipticity parameter is given as $\epsilon \simeq 0.2$. The parameter ω is determined to fit the value of the field.⁶ In Fig. 4 (the left figure), we present the fitted line with $\epsilon = 0.2$, $\omega = 1.149$ as the gray dashed line. The blue line is the same as the line in Fig. 1.

From the above solution, let us calculate the charge density profile. In Fig. 4 (the right figure), the gray dashed line is the result of the solution with the same parameters, $\epsilon = 0.2$, $\omega = 1.149$. The blue line is the same as the line in Fig. 2. We confirm the good agreement between the semi-analytic solution in method 1 and the simulation result.

⁶ The field value of the Q-ball center is sensitive to the value of ω .

We also calculate E/Q for ϵ to compare the result in Fig. 3. In Fig. 5, the gray dotted line is the result for $Q = 50$. We also confirm the good agreement with the simulation result.

Therefore, we find that method 1 is useful for the discussion on the properties of the elliptical Q-ball.

B. Method 2: Gaussian approximation

In method 1, we obtained the dispersion relation of the elliptical Q-ball by assuming the elliptical orbit in the complex plane. However, we can not obtain the information on the actual orbit of ϕ which satisfies the equation of motion.

In the following method, let us assume the spatial Gaussian profile of the elliptical Q-ball.

We also start from the expression of the energy of the complex scalar with the gravity-mediation potential in Eq. (3). Although we have to solve the equation of motion for both t and r , we approximate the spatial profile as Gaussian:

$$\phi(t, \mathbf{x}) = \varphi(t)e^{-r^2/R^2}, \quad (36)$$

where $\varphi(t)$ is a complex function of t . This Gaussian approximation is consistent with the result of method 1. We decompose $\varphi(t)$ into the radial direction $\Phi(t)$ and the phase direction $\theta(t)$:

$$\varphi(t) = \frac{1}{\sqrt{2}}\Phi(t)e^{i\theta(t)}. \quad (37)$$

Here we do not specify the time-dependence of $\Phi(t)$ and $\theta(t)$.

Then, the energy of the system is rewritten as

$$E = \int d^3x \left[\frac{1}{2}\dot{\Phi}^2 + \frac{1}{2}\dot{\theta}^2\Phi^2 + \frac{1}{2}\left(\frac{2r}{R^2}\right)^2\Phi^2 + \frac{1}{2}\Phi^2 \left[1 + K \ln\left(\Phi^2 e^{-2r^2/R^2}\right)\right] \right] e^{-2r^2/R^2}. \quad (38)$$

Performing the integration with respect to the spatial coordinate, we get

$$E = \frac{1}{2\sqrt{2}}\pi^{3/2}R^3 \left[\frac{1}{2}\dot{\Phi}^2 + \frac{1}{2}\dot{\theta}^2\Phi^2 + \frac{1}{2R^2}\Phi^2 + \frac{1}{2}\Phi^2 \left[1 + K \ln\left(\Phi^2 e^{-3/2}\right)\right] \right]. \quad (39)$$

Since the system conserves the $U(1)$ charge, the following relation is obtained

$$\int d^3x \dot{\theta}\Phi^2 e^{-2r^2/R^2} = \frac{1}{2\sqrt{2}}\pi^{3/2}R^3\dot{\theta}\Phi^2 = Q \text{ (constant)}. \quad (40)$$

Using the above relation in Eq. (40), the energy of the system is represented only by the radial direction:

$$\tilde{E} = \frac{1}{2}\dot{\Phi}^2 + U(\Phi), \quad (41)$$

where $U(\Phi)$ is an effective potential,

$$U(\Phi) = \frac{1}{2}\frac{\tilde{Q}^2}{\Phi^2} + \frac{1}{2R^2}\Phi^2 + \frac{1}{2}\Phi^2 \left[1 + K \ln\left(\Phi^2 e^{-3/2}\right)\right] \quad (42)$$

and we define $\tilde{E} = 2\sqrt{2}E/\pi^{3/2}R^3$ and $\tilde{Q} = 2\sqrt{2}Q/\pi^{3/2}R^3$.

This system is analogous to the Keplerian motion of the planet in the gravitational potential. The lowest energy state described in this system is apparently (see Fig. 6)

$$\text{(Ground state)} \quad \dot{\Phi} = 0, \quad \Phi = \Phi_0 \simeq \tilde{Q}^{1/2}, \quad (43)$$

where Φ_0 is a minimum of the effective potential and we use $R^{-2} \sim |K| \ll 1$. In this case, $\dot{\theta} = Q/\Phi_0^2 = \text{constant}$ and the φ describes the circular orbit in the complex plane. This solution is nothing but the ground-state Q-ball solution. Then, the energy per unit charge is given by

$$E_{\text{ground}}/Q = U(\Phi_0)/Q \simeq 1, \quad (44)$$

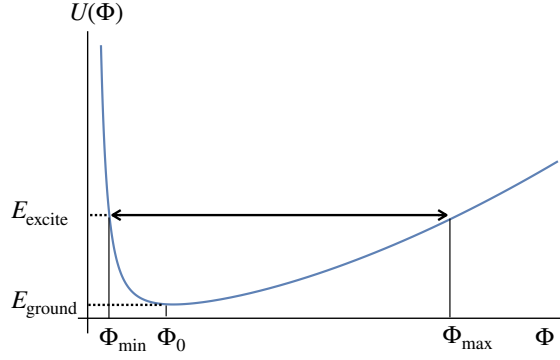


FIG. 6. The effective potential for Φ .

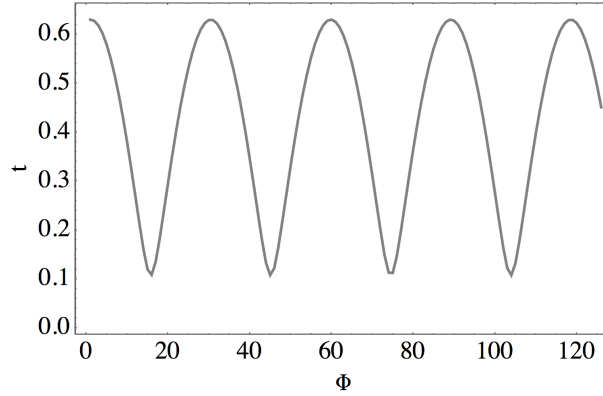


FIG. 7. The oscillation of Φ for $Q = 50$, $K = -0.1$, $R = 1/\sqrt{2|K|}$.

which is consistent with the result of a conventional formulation of the Q-ball Eq. (21).⁷

To obtain the excited state solution, let us consider the case $\dot{\Phi} \neq 0$ in the system. Because Φ obtains the kinetic energy, Φ oscillates around the potential minimum Φ_0 (Fig. 7).

In such a condition, the radial direction of the complex field ϕ oscillates between Φ_{\min} and Φ_{\max} , which means that the orbit of ϕ is elliptical. Due to the non-vanishing kinetic energy of Φ , the energy of this Q-ball is larger than circular (ground state) Q-ball (Fig. 7):

$$E_{\text{excite}}/Q = U(\Phi_{\min})/Q = U(\Phi_{\max})/Q \gtrsim 1. \quad (45)$$

Since Φ_{\min} and Φ_{\max} are related to the ellipticity parameter as $\epsilon = \Phi_{\min}/\Phi_{\max}$, the ratio E/Q is calculated as a function of ϵ . Neglecting the contribution of the order $|K|$, we obtain

$$\tilde{E}_{\text{excite}} \simeq \frac{1}{2} \frac{\tilde{Q}^2}{\Phi^2} + \frac{1}{2} \Phi^2 \Leftrightarrow \Phi^2 = \begin{cases} \Phi_{\max}^2 = \tilde{E}_{\text{excite}}^2 + \sqrt{\tilde{E}_{\text{excite}}^2 - \tilde{Q}^2} \\ \Phi_{\min}^2 = \tilde{E}_{\text{excite}}^2 - \sqrt{\tilde{E}_{\text{excite}}^2 - \tilde{Q}^2} \end{cases} \quad (46)$$

Therefore,

$$\epsilon^2 = \frac{\tilde{E}_{\text{excite}}^2 - \sqrt{\tilde{E}_{\text{excite}}^2 - \tilde{Q}^2}}{\tilde{E}_{\text{excite}}^2 + \sqrt{\tilde{E}_{\text{excite}}^2 - \tilde{Q}^2}} \rightarrow E_{\text{excite}}/Q \simeq \frac{1 + \epsilon^2}{2\epsilon}, \quad (47)$$

⁷ Strictly speaking, this relation has a little dependence on Q of order $|K|$.

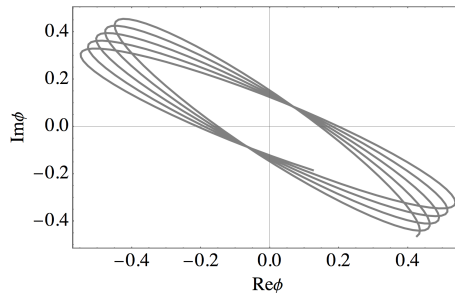


FIG. 8. The orbit of the ϕ for the excited Q-ball for $Q = 50$, $R = 1/\sqrt{2|K|}$.

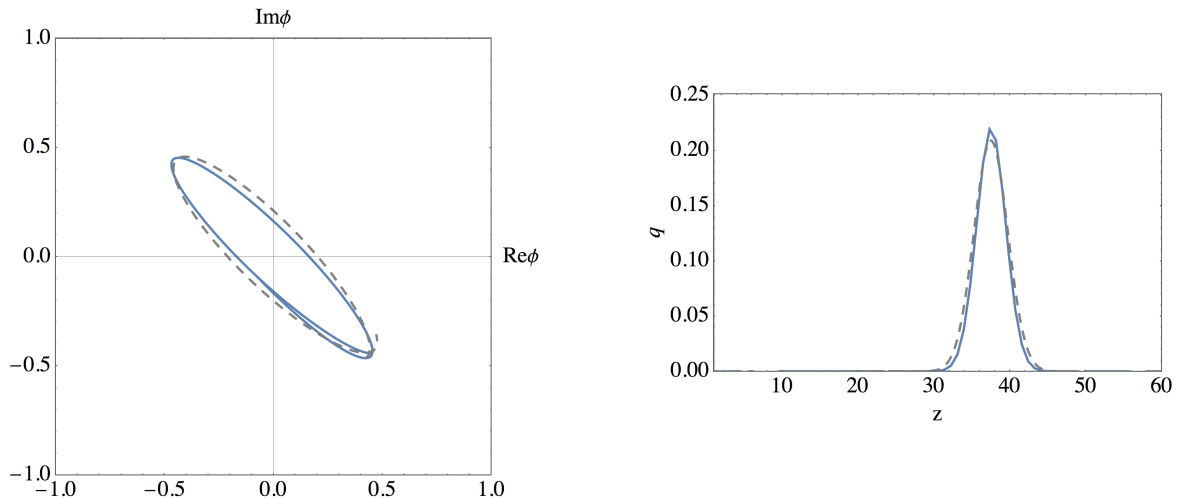


FIG. 9. Fitting in method 2. The gray dashed line is the orbit and the charge density profile from method 2 in the left and the right figures, respectively. The blue line is the same as the one in Fig. 1. Here, we take $Q = 36.5$, $R = 4.46$.

which is consistent with the one derived in method 1 in Eq. (34).

Finally, we show the orbit of ϕ in the complex plane in Fig. 8. There, we take $Q = 50$, $R = 1/\sqrt{2|K|}$. We can see that the axis of the ellipse is rotating in time. Therefore, the perfect ellipse assumption in method 1 holds only approximately. While method 2 can describe the orbit in the complex plane accurately, it does not give us information about the spatial profile of the elliptical Q-ball. On the other hand, although the method 1 cannot describe the orbit in the complex plane, it tells us the spatial profile of the elliptical Q-ball. As we will see later, both method 1 and 2 describe the elliptical Q-ball formed in the lattice simulation with good approximation.

Comparing with simulation result

In Fig. 9, we show the fitted lines for the orbit and the charge density. There, the gray dashed lines are the results by method 2 with $Q = 36.5$, $R = 4.46$. The blue lines are the same as the orbit and the charge density in Fig. 1 and Fig. 2. As in the case of method 1, we again confirm the good agreement between the semi-analytical solution in method 2 and the simulation results.

The ratio E/Q for ϵ is also calculated in method 2. We show the result from method 2 in Fig. 10. The gray dotted line is the result for $Q = 50$ (and $R = 5.8$). There, we also find a good agreement with the simulation results.

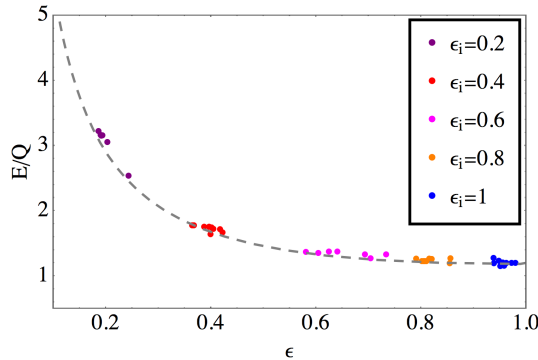


FIG. 10. The dispersion relations obtained from the lattice simulation and from method 2. The gray dotted line is E/Q for $Q = 50$. The data from the simulation is the same as that in Fig. 3. Here, we take $R = 5.8$.

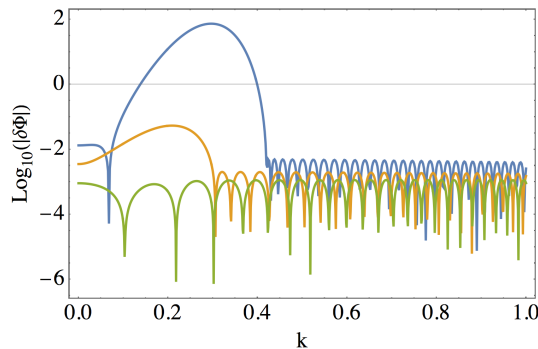


FIG. 11. The growth of $\delta\Phi$. The horizontal axis denotes the frequency k . The blue, orange, green lines correspond to the background elliptical Q-ball with $\epsilon = 0.2, 0.5, 0.8$, respectively. Here, we take $Q = 50$, $R = 1/\sqrt{2}$ for demonstration.

C. Stability of elliptical Q-ball

Before closing this section, let us briefly discuss the stability of the elliptical Q-balls.⁸ We know that the circular Q-ball $\epsilon = 1$ is absolutely stable because it is the most stable state which the complex scalar can take. In the case of the elliptical Q-balls, however, they might move to the more stable state, that is, less elliptical Q-balls. In fact, Ref. [14] observed the fission of the elliptical Q-ball to the multiple Q-balls, which are less elliptical than the original one. Therefore, the elliptical Q-balls are considered as the “transients”, which appear during the formation of the circular Q-balls.

The transition of the elliptical Q-balls to the mildly-elliptical Q-balls is well understood by our semi-analytical method. In method 2, let us consider a little perturbation $\delta\Phi$ around the elliptical Q-ball solution:

$$\Phi(\mathbf{x}, t) = \bar{\Phi}(t) + \delta\Phi(\mathbf{x}, t), \quad (48)$$

where $\bar{\Phi}$ is the background elliptical Q-ball solution which satisfies the equation of motion. Then, the equation of motion for the perturbation $\delta\Phi$ is

$$\delta\ddot{\Phi} + U''(\bar{\Phi})\delta\Phi = 0. \quad (49)$$

Solving this equation numerically, we can see that $\delta\Phi$ has instability and grows exponentially in time.

In Fig. 11, we show the growth of the instability for some elliptical parameter ϵ . There, we take $Q = 50$, $R = 1/\sqrt{2}$ for demonstration. The green, orange, blue lines denote the fluctuation $|\delta\Phi|$ for $\epsilon = 0.2, 0.5, 0.8$ after 300 oscillation of Φ , respectively. This is nothing but the broad resonance which is originated by the higher order self-coupling of the complex scalar.

⁸ Further details, *e.g.* compared with the simulation results, will be given in the forthcoming paper.

Therefore, for a certain time scale, the fluctuation $\delta\Phi$ dominates over the background mode $\bar{\Phi}$ and the original Q-ball solution is no longer maintained. After that, more stable configuration, that is, mildly excited Q-balls are produced. The time scale of such fission is considered to be related to the magnitude of the instability. If the amplitude of the oscillation of $\bar{\Phi}$ is larger, the instability becomes stronger and the fission of the elliptical Q-ball takes place for shorter timer scale. This means that highly-elliptical Q-ball has a short lifetime. In fact, Ref. [14] suggests that the fission of the elliptical Q-ball is efficient for highly-elliptical case $\epsilon \ll 1$.

V. CONCLUSION

In this paper, we have performed the simulation of the formation of the elliptical Q-balls. The elliptical Q-balls are inevitably produced in a realistic situation to compensate for the energy gap between the coherent state and the Q-ball state. We also formulated the elliptical Q-ball solution and derived its properties. We showed that they are in good agreement with the result of the lattice simulation. We have also shown that the elliptical Q-ball solution is unstable against the small perturbation. This implies that the elliptical Q-ball will decay into a more stable configuration, that is, mildly elliptical Q-balls in a finite time. For the stability of the elliptical Q-balls, further details will be given in a forthcoming paper, where we will also analyze the case of gauge mediation potential, etc.

Let us also comment on applications of our methods to other non-topological solitons, *e.g.* oscillon/I-ball [18–26] and boson star [27, 28]. As we have mentioned in the introduction, it is suggested that oscillon/I-ball and boson star are regarded as Q-ball solution associated with the particle number $U(1)$ charge [29, 30]. Therefore, it may be possible to derive some extended solutions of such non-topological solitons. These will also be explored in future work.

ACKNOWLEDGEMENTS

J.P.H is supported by Korea NRF-2015R1A4A1042542. The work of F.H. and M.S. is supported in part by a JSPS Research Fellowship for Young Scientists Grant Number 17J07391 (F.H.) and 18J12023 (M.S.)

-
- [1] S. R. Coleman, *Nucl. Phys.* **B262**, 263 (1985), [Erratum: *Nucl. Phys.*B269,744(1986)].
 - [2] I. Affleck and M. Dine, *Nucl. Phys.* **B249**, 361 (1985).
 - [3] A. G. Cohen, S. R. Coleman, H. Georgi, and A. Manohar, *Nucl. Phys.* **B272**, 301 (1986).
 - [4] M. Dine, L. Randall, and S. D. Thomas, *Nucl. Phys.* **B458**, 291 (1996), arXiv:hep-ph/9507453 [hep-ph].
 - [5] G. R. Dvali, A. Kusenko, and M. E. Shaposhnikov, *Phys. Lett.* **B417**, 99 (1998), arXiv:hep-ph/9707423 [hep-ph].
 - [6] A. Kusenko and M. E. Shaposhnikov, *Phys. Lett.* **B418**, 46 (1998), arXiv:hep-ph/9709492 [hep-ph].
 - [7] K. Enqvist and J. McDonald, *Phys. Lett.* **B425**, 309 (1998), arXiv:hep-ph/9711514 [hep-ph].
 - [8] K. Enqvist and J. McDonald, *Phys. Lett.* **B440**, 59 (1998), arXiv:hep-ph/9807269 [hep-ph].
 - [9] K. Enqvist and J. McDonald, *Nucl. Phys.* **B538**, 321 (1999), arXiv:hep-ph/9803380 [hep-ph].
 - [10] S. Kasuya and M. Kawasaki, *Phys. Rev.* **D61**, 041301 (2000), arXiv:hep-ph/9909509 [hep-ph].
 - [11] S. Kasuya and M. Kawasaki, *Phys. Rev.* **D62**, 023512 (2000), arXiv:hep-ph/0002285 [hep-ph].
 - [12] K. Enqvist, A. Jokinen, T. Multamaki, and I. Vilja, *Phys. Rev.* **D63**, 083501 (2001), arXiv:hep-ph/0011134 [hep-ph].
 - [13] S. Kasuya and M. Kawasaki, *Phys. Rev.* **D64**, 123515 (2001), arXiv:hep-ph/0106119 [hep-ph].
 - [14] T. Hiramatsu, M. Kawasaki, and F. Takahashi, *JCAP* **1006**, 008 (2010), arXiv:1003.1779 [hep-ph].
 - [15] K. Enqvist and J. McDonald, *Nucl. Phys.* **B570**, 407 (2000), [Erratum: *Nucl. Phys.*B582,763(2000)], arXiv:hep-ph/9908316 [hep-ph].
 - [16] M. S. Volkov and E. Wonnert, *Phys. Rev.* **D66**, 085003 (2002), arXiv:hep-th/0205157 [hep-th].
 - [17] M. V. Polyakov and P. Schweitzer, *Int. J. Mod. Phys.* **A33**, 1830025 (2018), arXiv:1805.06596 [hep-ph].
 - [18] I. L. Bogolyubsky and V. G. Makhankov, *Pisma Zh. Eksp. Teor. Fiz.* **24**, 15 (1976).
 - [19] M. Gleiser, *Phys. Rev.* **D49**, 2978 (1994), arXiv:hep-ph/9308279 [hep-ph].
 - [20] E. J. Copeland, M. Gleiser, and H. R. Muller, *Phys. Rev.* **D52**, 1920 (1995), arXiv:hep-ph/9503217 [hep-ph].
 - [21] S. Kasuya, M. Kawasaki, and F. Takahashi, *Phys. Lett.* **B559**, 99 (2003), arXiv:hep-ph/0209358 [hep-ph].
 - [22] M. A. Amin, R. Easther, and H. Finkel, *JCAP* **1012**, 001 (2010), arXiv:1009.2505 [astro-ph.CO].
 - [23] M. Gleiser, N. Graham, and N. Stamatopoulos, *Phys. Rev.* **D83**, 096010 (2011), arXiv:1103.1911 [hep-th].
 - [24] M. A. Amin, R. Easther, H. Finkel, R. Flauger, and M. P. Hertzberg, *Phys. Rev. Lett.* **108**, 241302 (2012), arXiv:1106.3335 [astro-ph.CO].
 - [25] K. D. Lozanov and M. A. Amin, *Phys. Rev.* **D97**, 023533 (2018), arXiv:1710.06851 [astro-ph.CO].
 - [26] P. Salmi and M. Hindmarsh, *Phys. Rev.* **D85**, 085033 (2012), arXiv:1201.1934 [hep-th].
 - [27] D. J. Kaup, *Phys. Rev.* **172**, 1331 (1968).

- [28] R. Ruffini and S. Bonazzola, *Phys. Rev.* **187**, 1767 (1969).
- [29] K. Mukaida and M. Takimoto, *JCAP* **1408**, 051 (2014), [arXiv:1405.3233 \[hep-ph\]](#).
- [30] J. Eby, K. Mukaida, M. Takimoto, L. C. R. Wijewardhana, and M. Yamada, (2018), [arXiv:1807.09795 \[hep-ph\]](#).
- [31] T. D. Lee and Y. Pang, *Phys. Rept.* **221**, 251 (1992), [,169(1991)].
- [32] J. Sainio, *JCAP* **1204**, 038 (2012), [arXiv:1201.5029 \[astro-ph.IM\]](#).